A REAL TIME CAMERA SYSTEM FOR DISASTER AND TRAFFIC MONITORING

F. Kurz[*], D. Rosenbaum, J. Leitloff, O. Meynberg, P. Reinartz

German Aerospace Center (DLR), Remote Sensing Technology Institute, PO Box 1116, D-82230 Weßling, Germany
franz.kurz@dlr.de

ABSTRACT:
A real time airborne monitoring system for monitoring of natural disasters, mass events, and large traffic disasters was developed in the last years at the German Aerospace Center (DLR). This system consists of an optical wide-angle camera system (3K system), a SAR sensor, an optical and microwave data downlink, an onboard processing unit and ground processing station with online data transmission to different end user portals. The development of the real time processing chain from the data acquisition to the ground station is still a very challenging task. In this paper, an overview of all relevant parts of the airborne optical mapping system is given and selected system processes are addressed and described in more detail. The experiences made in the flight campaigns of the last years are summarized with focus on the image processing part, e.g. reached accuracies of georeferencing and status of the traffic processors.

1. AIRBORNE RAPID MAPPING

Real time monitoring of natural disasters, mass events, and large traffic disasters with airborne optical sensors is a focus of research and development at the German Aerospace Center (DLR) since several years. Rapid mapping for natural disasters was long time the domain of satellite images which were processed and distributed by institutions like the ZKI[1] (Center for Satellite Based Crisis Information). Airborne rapid mapping can fill a gap as satellites are fixed to overpass times and are thus not available at any time. Besides, airplanes can be directed flexibly with a high spatial and temporal resolution.

Ongoing projects at DLR (VABENE[2], SAFER (E.U.), etc.) try to fill this gap and enforce the use of airborne rapid mapping for different applications. In these projects, airborne rapid mapping systems are developed and tested together with end users like the national rescue forces and security related forces (BOS) (Kurz et al., 2009). In the VABENE project, different end users portals are developed and the forces are equipped with powerful tools like the DMT (Disaster management tool), which provides direct and mobile access to airborne images and traffic data.

Traffic data are distributed by the EmerT-Portal. Here, terrestrial traffic data are fused with airborne acquired traffic data. Special tools like traffic prognosis and traffic routing for emergency forces are available.

Orthophoto maps with additional info layers are distributed by the ZKI Portal. Here, printed maps are distributed, which are very useful for rescue forces as often no computers are available at all times in crisis situations.

The development of these systems is in close contact with the German national rescue and security related forces.

In this paper, an overview of all relevant parts of the airborne rapid mapping system is given and selected system processes are addressed and described in more detail. The experiences made in the flight campaigns of the last years are summarized with focus on the image processing part, e.g. achieved accuracies of georeferencing and traffic data processing.

---

[1] http://www.zki.dlr.de/
[2] http://vabene.dlr.de

2. SYSTEM HARDWARE

2.1 DLR 3K camera system

There are two sensor units operated, the 3K and 3K+ camera system licensed for the DLR airplanes Cessna and Do228 (Kurz 2007; Reinartz 2006). Most important components of the DLR 3K camera systems are the cameras, which are described in more detail in this chapter.

Each system consists of three non-metric Canon cameras, for the 3K system the Canon EOS 1Ds Mark II camera with 50mm Canon lenses is used whereas the successor model 3K+ uses CANON EOS 1Ds Mark III cameras with 50mm Zeiss lenses. The 3K and 3K+ systems are mounted on a ZEISS aerial shock mount ready for the DLR airplanes (see Figure 1).

Figure 1: The 3K+ camera system

The main differences between 3K and 3K+ are the cameras and lenses, the rest of the hardware and software components are the same. The properties of the 3K and 3K+ systems are listed in Table 1. Most important issue is the higher resolution of the 3K+, as the Mark III camera delivers 21.0MPix compared to 16.7MPix of the Mark II camera. The theoretical resolution of 3K resp. 3K+ from 1000m a.g. is then 15cm resp. 13cm in nadir direction. The Mark III camera also outperforms the Mark II in the higher frame rate and the maximum number of images,

which is important for photogrammetric applications where high image overlaps are necessary. The Mark III offers 5Hz maximum frame rate resulting e.g. in 97% overlap at 1000m a.g. Due to the improved performance of the Mark III, the camera takes up to 63 images with 5Hz[3]. The number of images is limited due to an overflow of the internal memory, which depends on the data rate at the cameras. The listed data rates 8.3 resp. 9.8 MByte/s at 0.5Hz can be used for unlimited continuous acquisition. Therefore, different acquisition modes are required depending on the application.

	3K	3K+
Cameras	3 × EOS 1Ds Mark II	3 × EOS 1Ds Mark III
Sensor / Pixel size	Full frame CMOS / 7.21µm	Full frame CMOS / 6.41µm
Image size	3 × 4992 × 3328 (16,7MPix)	3 × 5616 × 3744 (21,0 MPix)
Max. fps (Max. images)	3 Hz (~50 images)	5Hz (63images)
File size	20MByte (RAW) 5,5MByte (JPEG level 8)	25MByte (RAW) 6,5 MByte (JPEG level 8)
ISO	100 – 1600	50 – 3200
Aperture	1.4 – 22	1.4 – 22
Lenses	Canon EF 1.4 50mm	Zeiss Makro-Planar 2/50mm
Data rate (JPEG level 8) at 0.5Hz	8,3MByte/s	9,8MByte/s
Interface	Firewire IEEE 1394a	USB 2.0

Table 1 Properties of 3K and 3K+ camera system

Typical flight heights of the camera systems lie between 500m and 3000m above ground. The GSDs reach from 6.5cm till 45cm not including forward motion blurring and other effects. In Table 2, all relevant properties of the viewing configurations are listed based on 50mm lenses. The viewing directions of the sideward looking cameras of 3K/3K+ are variable up to 32°. The FOV at the maximum angle is 104° along track and 26° across track. The coverage is defined as bounding box of orthorectified images from all three cameras assuming horizontal airplane orientation.

	3K	3K+
Viewing directions	Max 32° /variable	Max 32° / variable
FOV	104° across, 26° along	104° across, 26° along
Coverage / GSD @ 500m a.g.	1280m × 240m / 7.5cm nadir	1280m × 240m / 6.5cm nadir
Coverage / GSD @ 1000m a.g.	2560m × 480m / 15cm nadir	2560m × 480m / 13cm nadir
Coverage / GSD @ 3000m a.g.	7680m × 1440m / 45cm nadir	7680m × 1440m / 39cm nadir

Table 2: Properties of the different viewing configurations

2.2 Real time processing units

For real time processing of 3K-camera images a distributed airborne image processing system is currently developed by DLR (see Figure 2), consisting of up to five PCs or Laptops onboard. Each camera is connected via USB or firewire to a PC which is responsible for image acquisition, for the orthorectification of images, and for the street segmentation as part of the traffic processor. Data are collected at the fourth PC, which is responsible for vehicle detection and vehicle tracking. The fifth PC collects all data and sends them to a ground antenna via a C-Band microwave link.

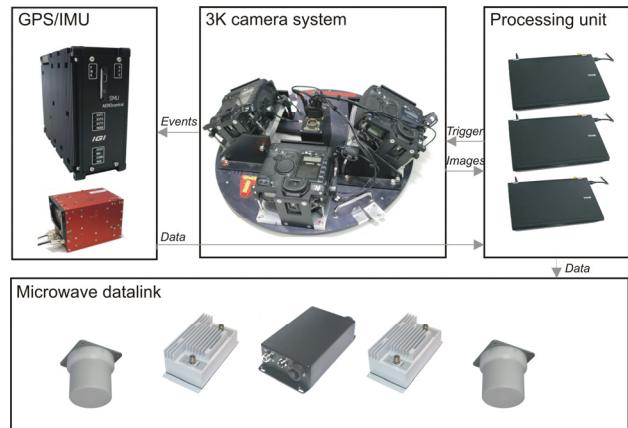3 Depending on the motif and other camera specific configuration parameters

Figure 2: Airborne hardware components and data flow of the 3K camera system for the real time processing chain

The data flow operates automatically without interaction. The cameras are triggered by PCs, and then the flash output of each camera triggers the GPS/IMU. Every time a flash signal is received, the GPS/IMU sends coordinates and orientation via a TCP connection to one of the camera PCs. A module runs a TCP client and matches the received geo-data with the image received from the camera. Together with a DEM and the calibration parameters, each image is orthoprojected by direct georeferencing. All modules are based on a proprietary architecture (Thomas, 2009).
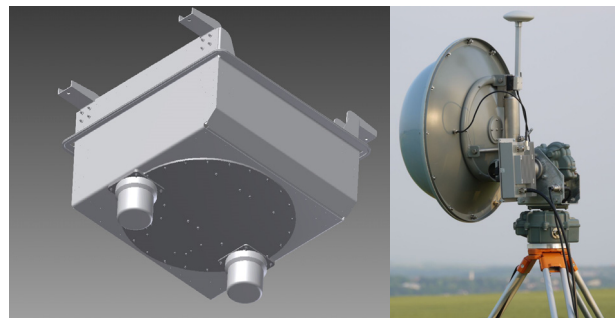
2.3 Microwave data downlink

Figure 3: Airplane antennas (left) and ground antenna (right)

Component	Size [mm]	Weight [kg]
2x Microwave antenna (SRS)	120×120×113	0.75
2× Amplifier (SRS)	78×108×220	1.60
1× Network radio (SRS)	58×120×230	1.00
1xGround Antenna	∅600	5.00kg
Data rate in the C-band / Range	40MBit/s for 100km	

Table 3: Technical parameters of the microwave datalink.

The processed data are transmitted to a ground station using a commercial autotracking microwave C-band downlink with a data rate of approx. 40Mbit/s and a range of 100km. Manufacturer of both antennas is SRS[4]. The technical data of the antenna system are provided in Table 3. Images of the airplane antenna and the ground antenna are shown in Figure 3.

4http://www.srsw.de

Different types of data can be sent lossless to the ground station via a TCP/IP connection.

2.4 Optical data downlink

For higher data rates an optical terminal is developed at DLR's Communication and Navigation Institute, which uses a laser as carrier wave. Thus, data rates of up to 1GBit/s from a distance of 90km could be reached. More details can be found here[5] (see also Figure 4).
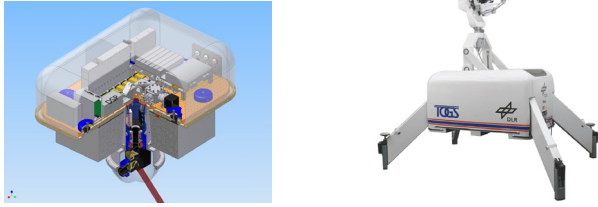

Figure 4: Airborne laser unit (left) and receiving station (right)

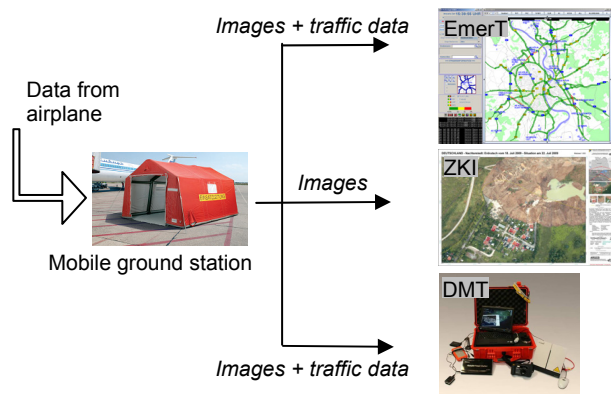## 2.5 Mobile ground station and data distribution

Figure 5: Data flow at the ground station

The mobile ground station consists of the microwave ground antenna, the ground part of the optical terminal, and data processing and validation infrastructure. If necessary, the ground station is moved close to the disaster area. For this purpose, a tent for the crew and for the technical infrastructure is set up. The processed and validated data are distributed to the end users using three portals: the EmerT-Portal for images and traffic data, the ZKI-Portal for images and classifications, and the DMT for images and traffic data. All three portals are mobile and autonomous, i.e. in case of failure of the public communication infrastructure the data flow will work autonomously as the data will be distributed directly from the mobile ground station.

The data flow is illustrated in Figure 5. For the EmerT-Portal, the user can access the image and traffic database by a web-based GUI. Here, the up-to-date traffic situation around the disaster area is visualized, the airborne images can be added as a layer, and different functions for route planning, travel time estimation and for other applications are implemented.

The ZKI-Portal is a user interface, which provides maps based on orthorectified airborne images. These maps can be printed to give them directly in the hands of the rescue forces. Additionally, classification layers like flood masks, burnt area masks etc. are added to the maps (example see Figure 6).

[5]http://vabene.dlr.de/vabene/opt_Data.htm

Figure 6: Example of ZKI map with flood layer

Last, data are distributed by the DMT (Disaster management tool). Here, the rescue forces are equipped with a case containing a GPS, camera, radio transceiver, and a small laptop. Airborne images are sent to the rescue forces in field by a datalink from the receiving device to the laptop. A software visualizes the images and shows the surrounding situation. Messages from other rescue forces can be read and every force can broadcast also messages with a time and position stamp (example see Figure 7).
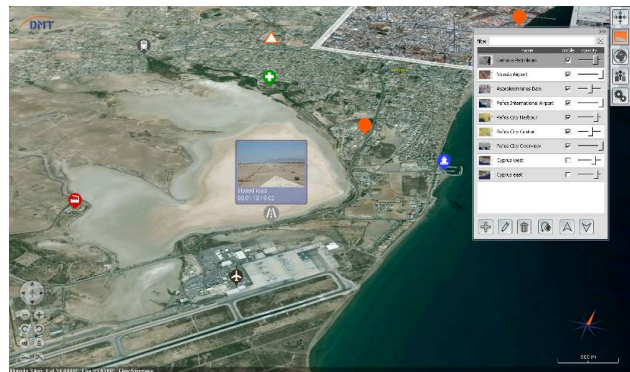

Figure 7: Screenshot of DMT software.

3. CAMERA PERFORMANCE

3.1 Orthophoto processing

The orthorectification is based on a straight forward georeferencing using the GPS/IMU data, the camera calibration data, and an on-board available digital elevation model.

Within the framework of the DGPF project for the evaluation of camera accuracies (Cramer, 2008), a data acquisition campaign at the test site in Vaihingen/Enz was conducted. The aim was to validate the accuracy of the 3K camera system at an independent test site. For this, a self-calibration bundle adjustment was performed on these data to assess the accuracy properties of the camera system and to (re)determine the interior parameters of the camera. The flight campaign was performed on 15th of July 2008. Table 4 lists the result of the accuracy of the 3K camera system at 61 check points (Kurz, 2009).

	Empirical RMSE (at 61 points)		Empirical RMSE (without systematics)
X	0.647 m	Max -1.166 m	0.331 m
Y	0.651 m	Max -1.787 m	0.380 m
Z	0.576 m	Max -1.702 m	0.527 m

Table 4. Accuracy of the 3K camera system at check points

The accuracies reach 65cm in position and 58cm in height including systematic effects, whereas the accuracies reached by direct georeferencing are worse in the magnitude of 2-3 meters. Here, the IMU and the DEM accuracy, as well as the interior and boresight determination influence the accuracy.

3.2 Radiometric properties

Using normal amateur cameras for airborne acquisitions poses problems, as forward motion can only be reduced with small exposure times. Tests show that for the standard viewing configuration from 1000m above ground and using 50mm lenses exposure times of 1/2000s are quite satisfying. Smaller exposure times would increase image vignetting whereas by using longer exposure times the forward motion blurring increases. Figure 8 shows the resolution of 3K and 3K+ images taken from 1000m a.g. at a flight speed of about 70m/s. Based on the Siemens-star the geometrical resolution of the images can be calculated (from left): 18.6cm, 13.2cm, and 13.2cm. Please note, that the resolution of the 3K+ cameras lies close to the theoretical resolution of 13cm whereas the theoretical resolution of the 3K is about 15cm.

Figure 8: 3K and 3K+ images from a Siemens-star with fixed exposure time and variable aperture and ISO film speed.

Different aperture and film speed values were tested. Best results were obtained when using aperture values in the range of 4.0 till 11.0 as well as the ISO film speed below 800. The image noise increases drastically when using higher film speed values (see Figure 9).
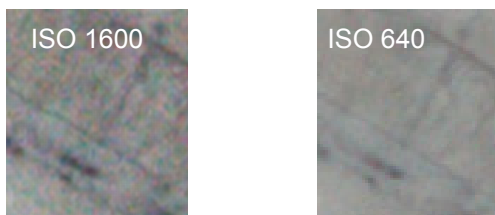

Figure 9: Comparison of different ISO film speeds.

4. TRAFFIC PARAMETER EXTRACTION

The traffic parameter extraction is based on three major steps: orthorectification of images, vehicle detection in selected road regions, and vehicle tracking. The methodology of traffic parameter extraction is described in detail in (Reinartz 2006, Rosenbaum 2008, Palubinskas 2009, Reinartz 2010, Leitloff 2010). In this chapter, the performance of this methodology is discussed and the accuracies of the obtained traffic parameters are validated.

4.1 Performance

Actuality of road traffic data is a general concern. For the use of aerial recorded data in the traffic simulation an actuality of less than five minutes is required. This means between exposure and receiving traffic data on the ground a maximum delay of five minutes is permitted. Hence, the processing chain must be optimized for processing speed. If traffic data extraction is limited to main roads, the bottle neck of the chain is produced by the orthorectification process that takes 10 to 12s for each nadir image. The actuality criterion is fulfilled for the first bursts of each flight strip easily, but a stack of unprocessed images is built up that leads to a critical length of the flight path. If the critical length is exceeded, the actuality criterion of the simulation will be overrun. This critical length of the flight path can be estimated. Taking into account a typical flight speed of 70m/s, three images recorded per burst, a break of 7s between each burst, the critical length is around 5km. In case of full traffic data extraction in urban centres the bottle neck moves to the traffic processor that slightly cannot keep up with the orthorectification performance (Figure 10).

Nevertheless, for road level of service visualization, the performance of the present processing chain is sufficient, since the hard actuality criterion of the simulation does not apply in this case. However, the present processing chain holds potential for improvement of calculation time, even for the orthorectification process.
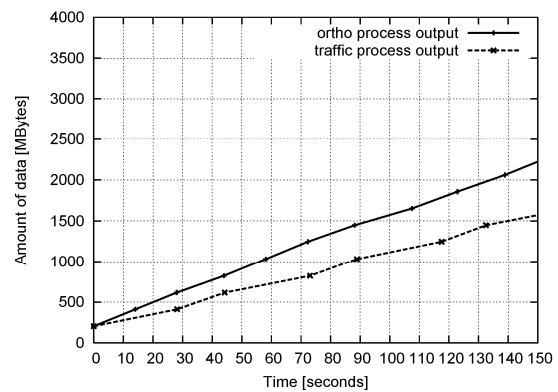

Figure 10: The diagram shows the amount of data which is processed by the Ortho Module but not by the Traffic Processor in case of full traffic data extraction including all road categories and urban centre scenarios.

4.2 RESULTS AND ACCURACY

The quality of traffic data obtained from the processing chain was evaluated on image sequences obtained on campaigns in Germany in the cities of Cologne and Munich. The Cologne image data were used for validating detection accuracy, whereas the Munich data were used for evaluating the tracking performance. The data represent a mix of scenarios ranging from urban centres and suburban roads to motorways. Due to the higher complexity of the scenes, the quality of traffic data extracted in metropolitan centres is somewhat lower than on motorways and suburban areas. This influences the vehicle detection notably. Therefore, the quality of vehicle detection is examined while distinguishing between these different scenes. However, each campaign contains a mixture of both scenes, since German city centres are typically limited to a diameter of a few kilometres, even for major German cities. Therefore, a total quality containing both scene types is listed as well, giving the typical quality of the detection to be expected in operational use.

The evaluation of tracking distinguishes between the two campaigns in Munich, since the weather and illumination conditions were different.

Table 5 shows the results of the vehicle detection algorithm. With a value of around 90% correctness the performance is at a very high level in all scenarios. In urban centres, the correctness drops slightly to 87%. The completeness with 93% in suburban and motorway scenes and 92% in total is at a very high level, providing precise estimates of local traffic density for traffic simulations or road level of service visualization. In urban centre regions it drops a little to a value of 90%. This results in a total quality of 83%.

Scene	Suburban & Motorways	Urban Core	Total
Images evaluated	73	6	79
True Positives	5545	2911	8456
False Positives	613	429	1042
False Negatives	424	317	741
Correctness	90%	87%	89%
Completeness	93%	90%	92%
Quality	84%	80%	83%

Table 5: Evaluation of vehicle detection

Table 6 presents the results of evaluating the vehicle tracking algorithm. The underlying image database represents a mix of urban centre and suburban/motorway scenes. Tracking performs well with a correctness of about 93% and a completeness of 97%. There is nearly no difference between the results obtained from two flights at different dates indicating that the tracking algorithm is robust against slight changes in weather and illumination conditions.

Scene	Munich 1	Munich 2	Total
Image series evaluated	29	19	48
True Positives	1002	724	1726
False Positives	75	47	122
False Negatives	36	23	59
Correctness	93%	94%	93%
Completeness	97%	97%	97%
Quality	90%	91%	91%

Table 6: Evaluation of vehicle tracking quality

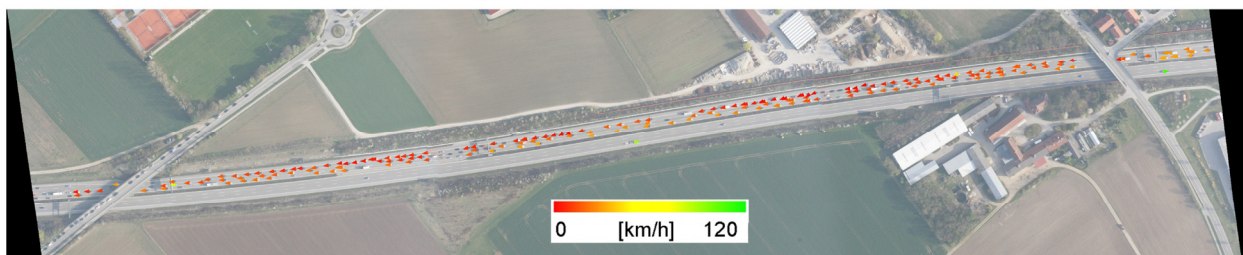The system accuracy is the product of detection and tracking quality. In the present case it is about 75%. This makes the system accuracy competitive to that of ground based sensor networks. The quality of a typical induction loop is better than 90% at time of production. During years of continuous operation it decreases slowly. In a complete sensor network of a metropolitan area there is a mix of new and older sensors, and some of them have even failed completely. This drops down the average quality or system accuracy of the sensor network. In Munich, the system accuracy of the complete ground based sensor network for traffic data acquisition has a value of 80%, as stated by Munich integrated traffic management centre.

The quality of traffic data obtained by the presented remote sensing system is shown to be competitive to that of road sensor networks in connection with the good spatial resolution (including minor roads) and the reliability in case of ground damage makes the system well suited for its operation during mass events and disasters.

5. CONCLUSIONS

Airborne rapid mapping for disaster and traffic monitoring is an interesting research field and technically challenging. The overall processing chain is on the edge of technical feasibility with respect to the data rates at the camera, the processing units in the airplane, and the data downlink. The focus in the development lies in the increase of the processing speed, the optimization of hardware prices, weights and volume, and the improvement of the software. As demonstrated, with amateur cameras quite respectable results regarding radiometric and geometric properties can be obtained.

When comparing the downlink data rate of 40MBit/s with the data rate at the cameras of around 100MBit/s, the need for data reduction as well as for accelerated algorithms by onboard processing becomes quite visible. This can be achieved by exploiting fast graphics hardware as it is investigated for orthorectification currently.

For traffic parameters extraction, the overall system quality is around 75% which is comparable to ground based sensors. Further improvements will include the detection of trucks as well as lane precise detection and special tracking for urban crossings and other complex traffic situations.

Figure 11: Traffic data extracted automatically by the processing chain near Munich. Quality of traffic parameter extraction is here ~80%.

6. LITERATURE

Cramer, M. (2010). The DGPF-Test on Digital Airborne Camera Evaluation – Overview and Test Design. PFG – Photogrammetri*e – Fernerkundung – Geoinformation* 2010/2, pp. 73-82. Germany

Kurz, F., Müller, R., Stephani, M., Reinartz, P., Schroeder, M. 2007. Calibration of a wide-angle digital camera system for near real time scenarios. In: *ISPRS Hannover Workshop 2007, High* Resolution *Earth Imaging for Geospatial Information*, Hannover, 2007-05-29 - 2007-06-01, ISSN 1682-1777

Kurz, F. 2009. Accuracy assessment of the DLR 3K camera system. *In: DGPF Tagungsband, 18. Deutsche Gesellschaft für Photogrammetrie, Fernerkundung und Geoinformation. Jahrestagung*, 2009-03-24 - 2009-03-26, Jena. ISSN 0942-2870

Leitloff, J., Hinz, S., Stilla, U. 2010. Vehicle Detection in Very High Resolution Satellite Images of City Areas. I*EEE Transactions on Geoscience and Remote Sensing, 48 (7)*, Seiten 2795-2806. The Institute of Electrical and Electronics Engineers, Inc. DOI: 10.1109/TGRS.2010.2043109. ISSN 0196-2892.

Palubinskas, G., Kurz, F., Reinartz, P., 2009. Traffic congestion parameter estimation in time series of airborne optical remote sensing images. In: *Proc. of ISPRS Hannover Workshop 2009 - High Resolution Earth Imaging for Geospatial Information*, 2-5 June, 2009, Hannover, Germany, ISPRS.

Reinartz, P., Lachaise, M., Schmeer, E., Krauss, T., Runge, H., 2006. Traffic monitoring with serial images from airborne cameras, *ISPRS Journal of Photogrammetry & Remote Sensing 61 (2006)*, 149-158.

Reinartz, P., Kurz, F., Rosenbaum, D., Leitloff, J., Palubinskas, G. 2010. Image Time Series for Near Real Time Airborne Monitoring of Disaster Situations and Traffic Applications. *In: International Archives of Photogrammetry, Remote Sensing and Spatial Information Sciences,* 38 (part I/W4), Seiten 1-6. ISPRS Istanbul Workshop, 11.-13. Oct. 2010, Istanbul, Türkei.

Rosenbaum, D., Kurz, F., Thomas, U., Suri, S., Reinartz, P. 2008. Towards automatic near real-time traffic monitoring with an airborne wide angle camera system. *European Transport Research Review, 1,* Springer, ISSN 1867-0717.

Thomas, U., Rosenbaum, D., Kurz, F., Suri, S., Reinartz, P., 2009. A new Software/Hardware Architecture for Real Time Image Processing of Wide Area Airborne Camera Images. *Real-Time Image Processing Journal*, Springer-Verlag.